



Cite this: *Chem. Soc. Rev.*, 2015, 44, 7465

## Programmable chemical reaction networks: emulating regulatory functions in living cells using a bottom-up approach

Hendrik W. H. van Roekel,<sup>†ab</sup> Bas J. H. M. Rosier,<sup>†abc</sup> Lenny H. H. Meijer,<sup>†abc</sup> Peter A. J. Hilbers,<sup>ab</sup> Albert J. Markvoort,<sup>\*ab</sup> Wilhelm T. S. Huck<sup>\*d</sup> and Tom F. A. de Greef<sup>\*abc</sup>

Living cells are able to produce a wide variety of biological responses when subjected to biochemical stimuli. It has become apparent that these biological responses are regulated by complex chemical reaction networks (CRNs). Unravelling the function of these circuits is a key topic of both systems biology and synthetic biology. Recent progress at the interface of chemistry and biology together with the realisation that current experimental tools are insufficient to quantitatively understand the molecular logic of pathways inside living cells has triggered renewed interest in the bottom-up development of CRNs. This builds upon earlier work of physical chemists who extensively studied inorganic CRNs and showed how a system of chemical reactions can give rise to complex spatiotemporal responses such as oscillations and pattern formation. Using purified biochemical components, *in vitro* synthetic biologists have started to engineer simplified model systems with the goal of mimicking biological responses of intracellular circuits. Emulation and reconstruction of system-level properties of intracellular networks using simplified circuits are able to reveal key design principles and molecular programs that underlie the biological function of interest. In this Tutorial Review, we present an accessible overview of this emerging field starting with key studies on inorganic CRNs followed by a discussion of recent work involving purified biochemical components. Finally, we review recent work showing the versatility of programmable biochemical reaction networks (BRNs) in analytical and diagnostic applications.

Received 1st May 2015

DOI: 10.1039/c5cs00361j

[www.rsc.org/chemsocrev](http://www.rsc.org/chemsocrev)

### Key learning points

- (1) Distinguish between the foci of systems chemistry and synthetic biology
- (2) Understand molecular logic of cells using a bottom-up approach
- (3) Identify key regulations in cell-free circuits displaying higher-order temporal dynamics
- (4) Grasp the coupling of reaction and diffusion in spatial organisation
- (5) Indicate several applications of *in vitro* synthetic biology

<sup>a</sup> Institute for Complex Molecular Systems, Eindhoven University of Technology, P. O. Box 513, 5600 MB Eindhoven, The Netherlands.

E-mail: [a.j.markvoort@tue.nl](mailto:a.j.markvoort@tue.nl), [t.f.a.d.greef@tue.nl](mailto:t.f.a.d.greef@tue.nl)

<sup>b</sup> Computational Biology Group, Eindhoven University of Technology, P. O. Box 513, 5600 MB Eindhoven, The Netherlands

<sup>c</sup> Chemical Biology Group, Eindhoven University of Technology, P. O. Box 513, 5600 MB Eindhoven, The Netherlands

<sup>d</sup> Institute for Molecules and Materials, Radboud University, Heyendaalseweg 135, 6525 AJ Nijmegen, The Netherlands. E-mail: [w.huck@science.ru.nl](mailto:w.huck@science.ru.nl)

<sup>†</sup> These authors contributed equally.

## 1. Introduction

Cells are complex biochemical systems sustained by an underlying network of dynamic regulatory circuits and signal transduction pathways which are ultimately responsible for the basic functionality and robustness of life.<sup>1–3</sup> These biochemical networks are composed of thousands of chemical species that interact *via* nonlinear kinetic processes and dissipate chemical energy to achieve their function. In the last decade, impressive work in systems biology has revealed some of the design principles correlating the topology of biochemical circuits to the range of biological responses that can be produced by these networks.<sup>4,5</sup>



These studies have shown that chemical self-organisation—the process by which a dissipative (bio)chemical system of several

components becomes ordered in space and time—is a key factor determining the output of intracellular circuits.<sup>6–8</sup> Unfortunately,



**Hendrik W. H. van Roekel**

*Rik van Roekel received his MSc degree in Biomedical Engineering (2011) from Eindhoven University of Technology (TU/e, The Netherlands). He is currently pursuing a PhD degree in the field of synthetic biology under supervision of Prof. P. A. J. Hilbers and Dr T. F. A. de Greef at the same university. His research focuses on computational design of cell-free biochemical reaction networks and circuitry by combining mathematics, systems theory, bioinformatics and statistics with experimental findings.*



**Bas J. H. M. Rosier**

*Bas Rosier received his MSc degree in Biomedical Engineering in 2014 at TU/e and is currently a PhD candidate under supervision of Dr T. F. A. de Greef and Prof. Luc Brunsveld at the same university. In his research he uses DNA origami scaffolds as molecular breadboards to study the kinetic effects of multi-enzyme complexes and cascades.*



**Lenny H. H. Meijer**

*Lenny Meijer received her MSc degree in Biomedical Engineering (2014) at TU/e. During her Master's she performed several interdisciplinary internships and completed the graduate program with the Institute for Complex Molecular Systems (ICMS). Lenny started her PhD (2014) under the supervision of Dr. T. F. A. de Greef, Prof. P. A. J. Hilbers, and Prof. M. Merckx. Her research interests include the field of in vitro synthetic biology and systems biology.*



**Albert J. Markvoort**

*Albert Jan Markvoort is an Assistant Professor in the Computational Biology group and member of the Institute for Complex Molecular Systems at TU/e, where he received his MSc in Applied Physics and PhD in Computer Science. His main research interests focus on molecular simulation and computational modelling of various self-assembling and self-organizing systems.*



**Wilhelm T. S. Huck**

*Wilhelm Huck is Professor of Physical Organic Chemistry. He received his PhD (promoter Prof. David Reinhoudt) in 1997 from the University of Twente. After postdoctoral research with Prof. Whitesides at Harvard University, he took up a position in the Department of Chemistry at the University of Cambridge, where he was promoted to Reader (2003) and Full Professor of Macromolecular Chemistry (2007). In 2010 he moved to the Radboud*



**Tom F. A. de Greef**

*Tom de Greef obtained an MSc degree in Biomedical Engineering (2004) at TU/e and continued with a PhD in Chemistry (2009) in the group of Prof. E. W. Meijer and Prof. R. P. Sijbesma at the same university. In 2010 he was appointed group leader at the Institute for Complex Molecular Systems at the same university. His research interests range from systems chemistry to in vitro synthetic biology.*

*University Nijmegen to set up a new group to elucidate the influence of the cellular environment on complex reaction networks in cells. His ultimate goal is to create a synthetic cell.*



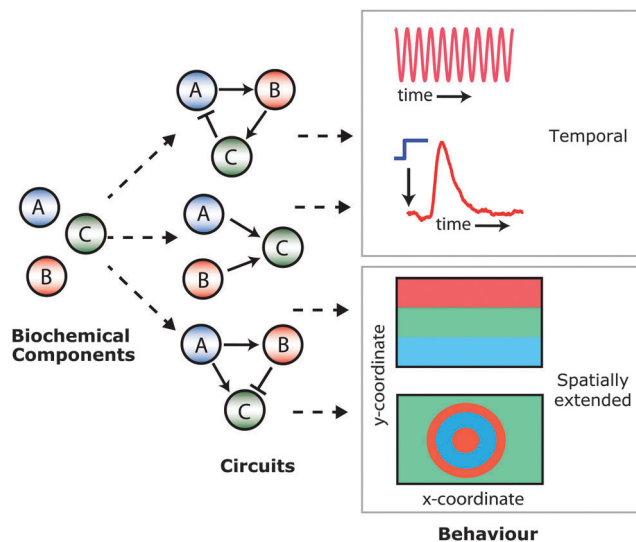


Fig. 1 Programmable cell-free biomolecular circuits built from modular biochemical components present a unique and uncharted platform to systematically explore the molecular logic and physical design principles of regulatory networks in the living cell. Complex (spatio)temporal behaviour exhibited by such circuits are based on elementary regulations such as activation and inhibition.

delineating the exact relation between biochemical network topology and the range of accessible spatiotemporal behaviours in living cells is not possible in many cases due to a limitation of current experimental tools.

One viable strategy to disentangle the complexity of cellular signalling networks is by applying a bottom-up approach, consisting of the construction of cell-free circuits that are able to display self-organising behaviours such as signal transduction, oscillations, self-replication, entrainment and programmed pattern formation (Fig. 1). Chemical self-organisation has been studied since the discovery of inorganic oscillators, such as the Belousov–Zhabotinsky (BZ) reaction in the 1960s. In the previous century, impressive work in this field led to a detailed understanding of the connection between feedback, diffusion and the emergence of complex self-organised behaviour such as chemical patterns and the ability of chemical systems to display higher-order dynamics such as oscillations and bistability.<sup>9</sup> These early studies on chemical self-organisation in relatively simple physicochemical systems have provided a new generation of physicists, chemists, and cell biologists with a comprehensive framework to tackle one of the key questions in science: to understand how living cells process information and control their global organisation using hierarchical layers of biochemical networks.<sup>4,6</sup>

These studies on self-organisation resulted in the rise of two related and partially overlapping fields, *i.e.* systems chemistry<sup>10</sup> and *in vitro* synthetic biology.<sup>11,12</sup> While systems chemistry focuses on the emulation of complex emergent phenomena encountered in living systems utilising a framework that is based on mostly abiotic homogeneous chemistry, *in vitro* synthetic biology is concerned with the bottom-up engineering of new and existing life-like functionalities using biological components. Both fields apply a bottom-up methodology to recapitulate the dynamic

organisation of living cells by replacing biology's complex and idiosyncratic regulatory networks by simpler and more predictable molecular circuitry. One of the key goals of *in vitro* synthetic biology is to reduce specific spatiotemporal functions of regulatory circuits in living cells to simple biochemical model systems. Using this approach, the relevant characteristics and interactions that determine the specific system-level behaviour of interest can be isolated and, importantly, mathematically described in a framework of simple theories. In addition, novel self-organisation principles employed by cells to receive, transmit and process stimuli into complex biochemical and physiological outputs can be discovered by stepwise increasing the complexity of these reductionist biochemical model systems.

For historical reasons and because of their prominent place within the field of chemical self-organisation, we start this Tutorial Review by highlighting key studies on engineered physicochemical systems based on the BZ reaction. Next, we review recent work on reconstituted and engineered enzymatic systems that display a wide range of self-organised temporal behaviours under well-stirred conditions such as bistability, oscillations and adaptation. However, in the intracellular environment, diffusion and crowding are fundamental drivers of spatiotemporal ordering. Therefore, we discuss several studies where programmed pattern formation and spatial information processing has been achieved using *in vitro* biomolecular systems. Finally, we review emerging applications of *in vitro* synthetic biology in the area of cell-free biosensing and diagnostics and material science.

## 2. Homogeneous inorganic reaction networks

Homogeneous chemical reaction networks (CRNs) that display dynamic self-organisation by coupling of reaction and diffusion have been studied since the second half of the 20th century. In CRNs coupling of feedback and diffusion can give rise to new behaviours. For example, autocatalysis – the process in which a reactant directly or indirectly drives the formation of itself – gives rise to global bistability in a well-stirred environment, while propagating fronts develop when the reaction is carried out in a quasi-two-dimensional unstirred setup. A system exhibits bistability when it is able to exist in two stable steady-states. Fig. 2A displays several topologies of autocatalytic networks while Fig. 2B displays bistability which can be triggered into one of the two possible steady-states using a stimulus. When appropriate negative feedback is introduced, the well-stirred setup becomes either excitable (*i.e.* an input above a certain threshold leads to a spike in the output before returning to the initial steady state) or oscillatory. In a spatially extended system, this leads to a single propagating pulse or a wave train of constant velocity, respectively. The BZ reaction was the first example of a class of inorganic chemical reactions that shows such out-of-equilibrium phenomena, *e.g.* bistability, and also oscillations and synchronisation (*vide infra*) that are visible to the naked eye.<sup>9</sup> Oscillations are signals in which temporal variations



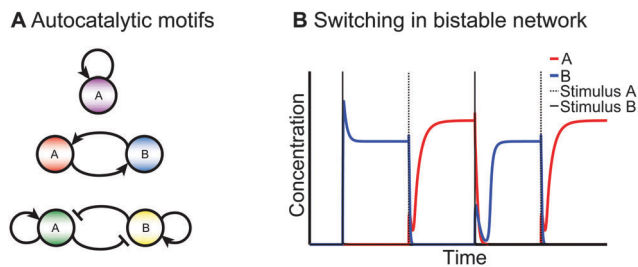


**Fig. 2** Autocatalysis and bistability. (A) Common autocatalytic motifs, with (top) direct autocatalysis, (middle) indirect autocatalysis and (bottom) mutual inhibition with autocatalysis. (B) An autocatalytic network that can exist in two steady states, *i.e.* one where A is dominant (red) and one where B is dominant (blue). Switching between these states is inducible by external stimuli.

about a central value occur with well-defined frequencies. The basic mechanism responsible for oscillations in the BZ reaction is the autocatalytic production of bromous acid ( $\text{HBrO}_2$ ) that is inhibited by bromide ( $\text{Br}^-$ ) *via* a delayed negative feedback mechanism (Fig. 3). This network motif is commonly encountered in other chemical and biochemical oscillators as well (*vide infra*). Moreover, the BZ reaction and equivalent inorganic CRNs are excitable by external stimuli. In the following, we discuss the BZ reaction and similar excitable inorganic reaction networks that can be triggered to display higher-order spatiotemporal behaviour, both in batch reactors and open chemostats. Furthermore, we highlight efforts to synchronise inorganic oscillators in space and time and finally discuss how these features make inorganic CRNs ideal emulators for life-like functionalities.

Excitability of the BZ reaction was first noted by Zaikin and Zhabotinsky in 1970,<sup>13</sup> when they found that a BZ reaction mixture dispersed as a thin layer in a Petri dish can be triggered

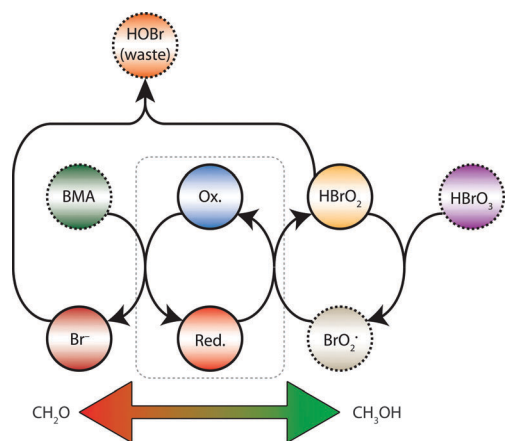


**Fig. 3** Key steps in the BZ reaction. The oxidation of the metal-ion catalyst (middle, enclosed with dashed box) is accompanied by conversion of  $\text{BrO}_2^*$  to  $\text{HBrO}_2$  resulting in an autocatalytic formation of  $\text{HBrO}_2$  (right). The reduction of the metal-ion catalyst (accompanied by the oxidation of BMA, left), produces  $\text{Br}^-$  that reacts with  $\text{HBrO}_2$ , serving as inhibition of the autocatalytic species under formation of waste product  $\text{HOBr}$ . The BZ reaction can be excited in a so-called activator-controlled mode by methanol, or in an inhibitor-controlled mode by formaldehyde, as these species slightly shift the balance to autocatalysis of  $\text{HBrO}_2$  or  $\text{Br}^-$  production, respectively.

into generating spatiotemporal waves originating from a single point called a pacemaker by perturbation of the medium. In an attempt to unravel the physicochemical principles that determine wave initiation, Bishop and Grzybowski<sup>14</sup> used wet stamping to deliver chemical stimuli from complex geometries to a gel containing the BZ reagents. This setup resulted in excitation of the system in a so-called activator-controlled mode, or inhibitor-controlled mode. Depending on the triggering agent present in the star-shaped stamp, *i.e.* formaldehyde for inhibitor-controlled mode (Fig. 4A) and methanol for activator-controlled mode (Fig. 4B), the autocatalytic step is initiated either in the star's tips or between the star's arms, resulting in focused wave emission. This phenomenon is explained by a slight shift in the balance between the activating and inhibiting perturbation, which is established by localised control of the autocatalytic process mainly by delivery or removal of the inhibitor species into or from the oscillatory region by diffusion. These diffusion processes are affected by the curvature of the star-shaped stamp and as a result, changing the triggering agent in the star directly affects the mode of wave emission from the star by inducing a spatiotemporal interplay between reaction kinetics and diffusion.

Rather than studying CRNs in batch reactors, the investigation of CRNs in an open-system setup prevents the ultimate decay of the reaction mixture towards thermodynamic equilibrium. Noszticzius *et al.*<sup>15</sup> studied the BZ reaction in an open-system with an experimental set-up that allows two solutions with BZ reactants to come into contact in an annular gel, resulting in initiation of the oscillatory reaction in the ring. Embedded with a pacemaker that triggers the reaction, and a wave barrier that attenuates counter clockwise waves, the system is instructed to generate waves with a defined frequency and direction. The resulting pattern resembles a pinwheel, Fig. 4C, as the distance between subsequent waves becomes constant. This study presents one of the first realisations of an open reactor in which the BZ reaction is excited into generating stable chemical patterns in time.

Open-system studies were taken to the next pioneering level in 2009, when De Kepper and co-workers<sup>16</sup> employed the iodate-sulfite reaction, which autocatalytically produces protons, to generate Turing-like patterns. The authors accomplished this by coupling the autocatalytic production of protons to a negative feedback on this autocatalytic loop by oxidation of an inhibitor species. Short-range spatiotemporal activation was realised by diffusive control of protons *via* reverse complexation to high-molecular weight ions, impairing their movement with respect to diffusion of the inhibitor. The resulting differential diffusivity of the inhibitor and the autoactivating species ensures long-range inhibition. A disc shaped spatial reactor takes up chemicals *via* diffusion on one face of the disc, resulting in pattern formation in the bulk of the disc. If the inhibitor exceeds a preset critical concentration, the inorganic CRN displays spatiotemporal self-organisation that is characteristic of a Turing bifurcation (the hexagonal patterns in Fig. 4D) in terms of localised low pH values. This study shows the possibility of higher-order spatiotemporal organisation by chemical reactions as a result of the judicious interplay of mass-transfer, reaction rates and



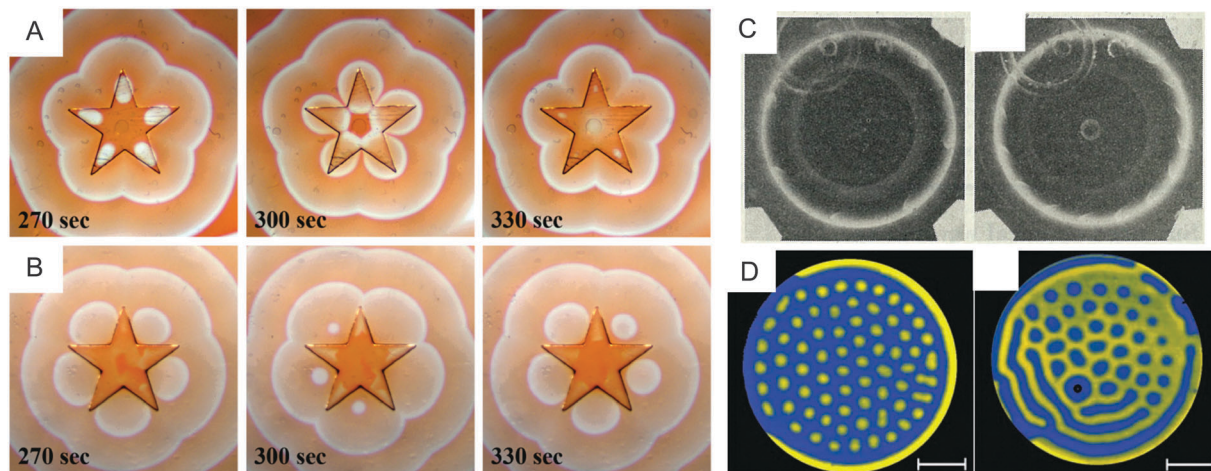


**Fig. 4** Excitability and spatiotemporal pattern formation in inorganic CRNs. (A) Inhibitor-controlled pattern formation and (B) activator-controlled pattern formation in the BZ reaction by a star-shaped stamp. Reprinted with permission from ref. 14 Copyright 2006 © American Physical Society. (C) Equidistant spatiotemporal waves resembling chemical pinwheels on an annular gel in which the BZ reaction takes place. Waves with a larger gap between them travel faster (left) than waves that are closer together (right). Reprinted with permission from ref. 15 Copyright 1987 © Macmillan Publishers Ltd. (D) Turing pattern formation in uncomplexed protons (yellow: low pH, blue: high pH) for high inhibitor concentration (left) and low inhibitor concentration (right). Reprinted with permission from ref. 16 Copyright 2009 © American Association for the Advancement of Science.

differential diffusivity of the components paving the way for future efforts aimed at engineering life-like biomolecular systems. Diffusion also plays an important organisational role on the  $\mu\text{m}$  scale in systems that operate with biological components (*vide infra*).

Model systems to investigate synchronisation by diffusive coupling were recently employed by the groups of Epstein<sup>17</sup> and Showalter.<sup>18</sup> Synchronisation is the process by which independent oscillators interact and assume the same temporal frequency. Epstein *et al.* investigated the communication between BZ droplets in oil *via* diffusive coupling by bromine employing a microfluidic set-up. The droplets showed out-of-phase synchronisation (Fig. 5A) and stationary Turing structures (Fig. 5B), depending on the droplet size and the initial concentration of malonic acid. The authors identified by experiment and by simulation that the inhibitor bromine is mainly responsible for communication between the droplets, as its hydrophobic character allows it to move between compartments. Therefore, bromine is responsible for the resulting synchronisation between droplets. Using a different approach, Taylor and Showalter *et al.* embedded microparticles with immobilised BZ catalyst and suspended the particles in a BZ reaction mixture lacking the catalyst. The experimental setup is displayed in Fig. 5C, along with a series of images showing a visibly changing synchronised population of microparticles during a single oscillation. The exchange rate of activator and inhibitor among the microparticles was controlled by the stirring rate of the suspension. At high exchange rates, the microparticles remain quiescent at low particle densities, and above a certain critical particle density, synchronised oscillatory behaviour is observed in a near step-wise fashion (graphs in Fig. 5C), reminiscent of the dynamics of quorum sensing. At low exchange rates, there is a linear increase of synchronisation with particle density, indicating that weak

coupling is the main mechanism of information exchange. The exchange of chemical information between BZ droplets or microparticles concerning their oscillatory state serves as a model system to rationalise global coupling of intracellular oscillators by intercellular cell-to-cell communication.

The studies discussed thus far provide key insights into the establishment of complex spatiotemporal dynamics *via* a bottom-up approach. We now stress the notion that inorganic CRNs can serve as useful model systems or even emulators for biological systems in several aspects. Firstly, all types of inorganic reactions discussed here are homogeneous reactions that maintain their far-from-equilibrium thermodynamic state for a significant amount of time, making them excellent functional model systems for non-equilibrium biological behaviour. Analogously, intracellular circuits use high-energy molecules to maintain steady-state transcription and translation rates. Secondly, biochemical synchronisation between living systems is observed in cell populations, *i.e.* quorum-sensing, which can be emulated by a suspension of microparticles. Finally, inorganic CRNs can be employed for information processing<sup>19</sup> and pattern storage<sup>20</sup> by excitable chemical systems, which could provide renewed insights on memory storage and decision making in intracellular networks where critical events such as cell-cycle progression and cellular differentiation are regulated by bistable network modules.

### 3. Temporal biochemical reaction networks

Recently, complex out-of-equilibrium behaviour has been established using biological macromolecules rather than small inorganic chemicals. This shift in approach allows the use of



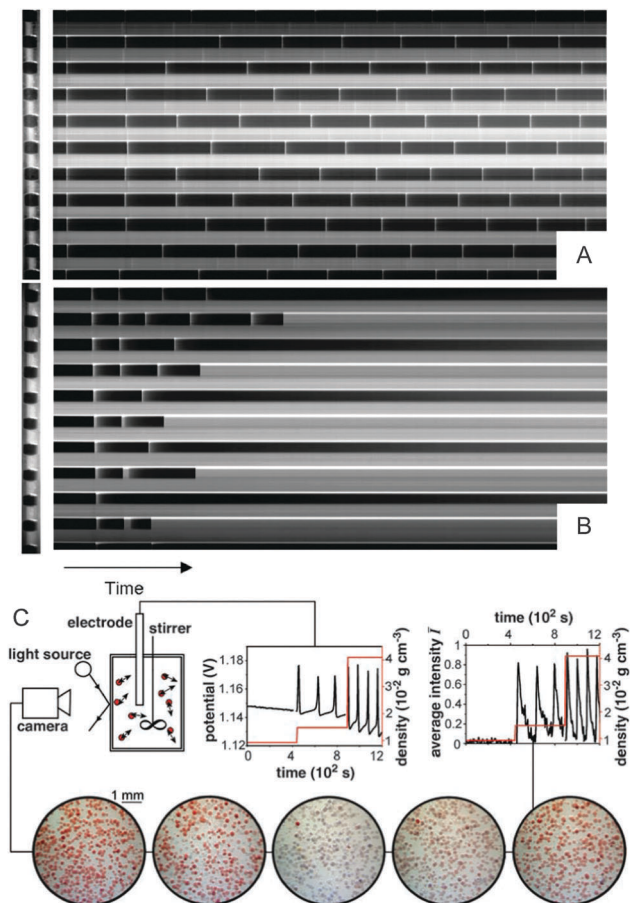


Fig. 5 Chemical synchronisation in the BZ reaction. (A) Space-time plot showing out-of-phase oscillations in a microfluidic set-up containing BZ droplets. (B) Space-time plot displaying stationary Turing patterns where the oxidised and reduced alternately appear from an initial oscillatory state. Reprinted with permission from ref. 17 Copyright 2008 © Wiley-VCH Verlag GmbH & Co. KGaA, Weinheim. (C) Experimental set-up for detecting quorum-sensing in a population of microparticles at high exchange rate: oscillations appear after a critical particle density. The bottom shows images of a single oscillation, visible as a colour change of the BZ catalyst immobilised on the beads. Reprinted with permission from ref. 18 Copyright 2009 © American Association for the Advancement of Science.

ambient conditions rather than the harsh acidic environments characteristic of the BZ reaction. In addition, CRNs based on biological molecules more closely resemble regulatory networks *in vivo*. Many pioneering studies conducted are concerned with the *in vitro* reconstitution of existing intracellular networks, such as oscillatory phosphorylation of KaiC by synergistic action of KaiA and KaiB.<sup>21</sup> Indeed, reconstruction of system-level properties of regulatory circuits using purified biochemical components can reveal key design principles and molecular programs that underlie the biological function of interest.<sup>22</sup> However, the focus of this Tutorial Review is on bottom-up rational design strategies to build cell-free model systems *de novo*. Therefore, we will focus on biochemical reaction networks (BRNs) that display various higher-order temporal functionalities including switching and oscillations. We limit the discussion to

enzymatically driven systems, *i.e.* those that rely on enzymes to maintain their thermodynamic nonequilibrium state. While non-enzymatic biomolecular networks are highly programmable and useful synthetic biological tools, intracellular networks use enzymatic reactions to achieve their function. Also, we refrain from discussing amplification reactions and amplifying cascades in this Tutorial Review.

In the previous section, bistable CRNs were briefly mentioned as core memory units. Indeed, living systems harness bi- and multistable molecular programs to store information concerning the state of a cell, and subsequently process this information to induce decision-making events. Kim, Winfree and co-workers<sup>23</sup> succeeded in the bottom-up design of an *in vitro* bistable enzymatically driven circuit based on synthetic DNA templates known as genelets that are regulated by RNA transcripts. The researchers developed the so-called genelet toolbox in which RNA polymerase (RNAP) transcribes RNA regulators from genelets that in turn serve as excitatory or inhibitory regulators for the transcription of RNA regulators from other genelets. In this way, the elimination of genes and their associated production and degradation of proteins that are not involved in the circuit allows for systematic analysis by means of a fairly accurate quantitative description that is impossible to achieve in *in vivo* systems or crude cell extracts. In Fig. 6A, the implementation of a genelet-based bistable switch is shown that consists of transcriptionally active and inactive double-stranded DNA (dsDNA) species and interacting RNA regulators. RNA regulators serve as inhibitors  $I_1$  and  $I_2$  of transcription from genelets  $Sw_{21}$  and  $Sw_{12}$ , respectively, by binding to the respective single-stranded DNA (ssDNA) activators  $A_1$  and  $A_2$ . Sequestration of activator DNA prevents formation of fully dsDNA resulting in a significant reduction of transcriptional activity. These reactions are designed to be very specific by appropriate choice of the base sequence. Activation is accomplished by degradation of RNA transcripts bound to the activator ( $A_i$ ) resulting in the release of the sequestered DNA activator. Fig. 6B shows the corresponding topology of the bistable BRN, while Fig. 6C displays the experimentally constructed bifurcation diagram with the two activator ssDNA concentrations ( $A_2^{\text{tot}}$  for  $Sw_{12}$  and  $A_1^{\text{tot}}$  for  $Sw_{21}$ ) as bifurcation parameters. Fig. 6D displays the switch activity time courses corresponding to high initial concentration of RNA inhibitor  $I_1$  (circles) or high initial concentration of RNA inhibitor  $I_2$  (lines). The system remains in the steady state that the investigators initiated, showing that two possible steady states exist. Further experiments to test the bistable circuit on hysteresis suggest that switching between steady states in a single experiment is possible at least once. The characterisation of individual genelets proved sufficient for the authors to assemble a bistable circuit, based on modularity and programmability of the components. The modularity of the genelet-toolbox have also allowed Kim, Murray and colleagues to assemble a synthetic transcriptional network that shows adaptation and fold change detection based on the incoherent feedforward loop (IFFL).<sup>24</sup>

Rondelez and co-workers<sup>25</sup> used a similar strategy to construct a bistable toggle switch, by introducing a modular toolbox by which biochemical networks of arbitrary complexity can be engineered *de novo* under well-controlled *in vitro* conditions.



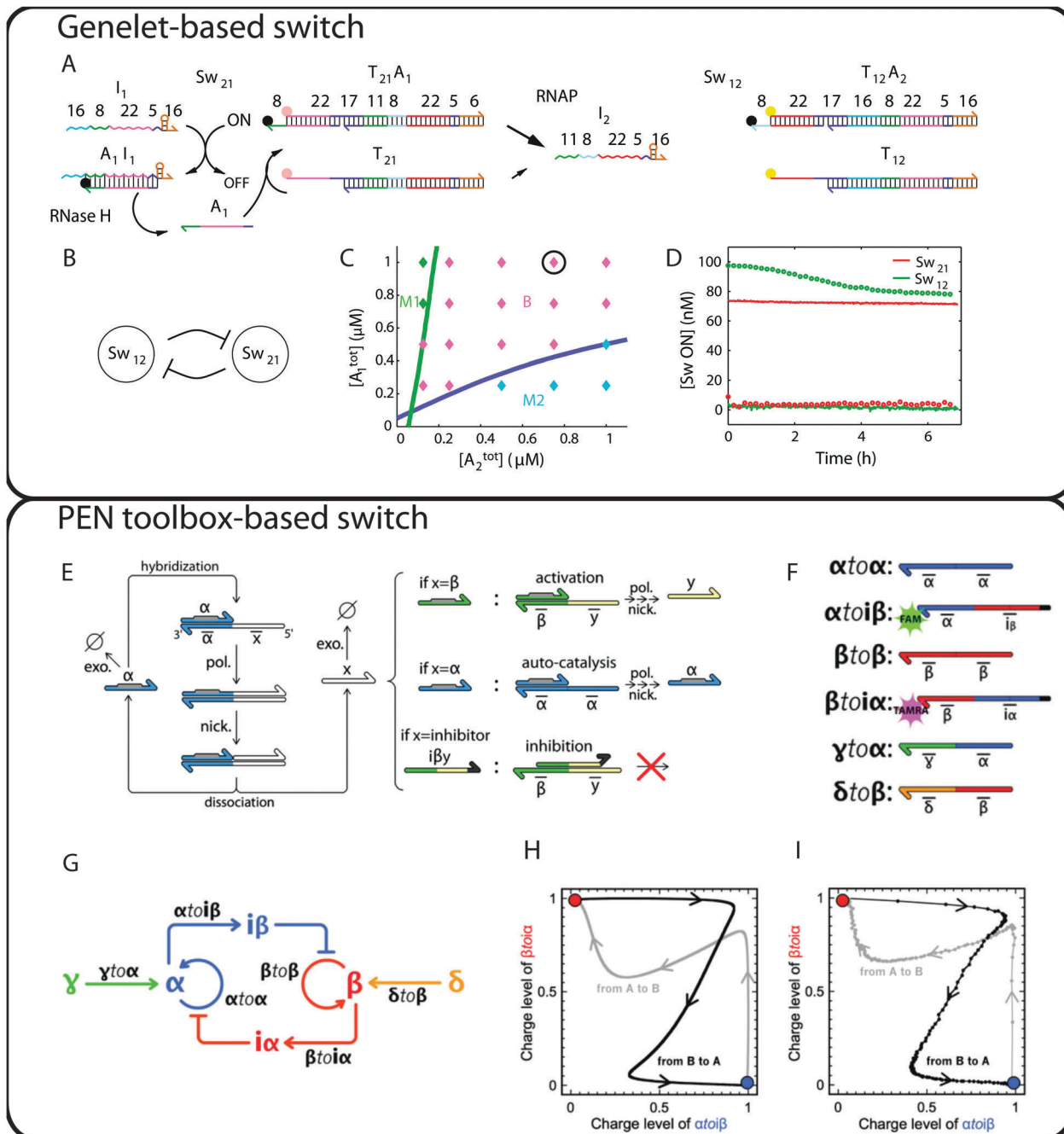


**Fig. 6** *In vitro* synthetic bistable switches. The top panel shows a genelet-based switch, and the bottom panel a polymerase–exonuclease–nickase (PEN) toolbox-based switch. (A) Implementation of the genelet-based switch based on synthetic template DNA from which RNA polymerase (RNAP) produces RNA regulators that in turn serve as excitatory or inhibitory regulators for the transcription of RNA regulators from other genelets, while RNase H degrades regulators from  $A_iI_i$  complexes. (B) Topology of the reaction scheme in A. (C) Experimentally constructed bifurcation diagram, with pink data points corresponding to bistable behaviour. (D) Switch activity time courses corresponding to the encircled data point in C, with high initial concentration of RNA inhibitor  $I_1$  (circles) or high initial concentration of RNA inhibitor  $I_2$  (lines). Reprinted with permission from ref. 23 Copyright 2006 © The authors (E) Reactions in the PEN toolbox: activator ssDNA  $\alpha$  primes the synthetic template, after which it is extended by DNA polymerase resulting in dsDNA. Nickase cleaves this dsDNA in the backbone of the newly formed strand, resulting in dissociation of signal strand  $X$ . Depending on the sequence of  $X$ , three types of reactions can occur, *i.e.* activation, autocatalysis and inhibition. (F) The six synthetic DNA templates of the bistable switch shown in G. (G) Topological representation of the PEN toolbox-based switch. The single-stranded input signals  $\gamma$  and  $\delta$  induce switching to the  $\alpha$  and  $\beta$  state, respectively. (H) Simulated predictions of switching to the  $\beta$  state by  $\delta$  (grey line) and of switching to the  $\alpha$  state by  $\gamma$  (black line). (I) A single switching experiment starting in the  $\alpha$  state, which is first switched to the  $\beta$  state by  $\delta$  (grey line), and subsequently switched back to the  $\alpha$  state by  $\gamma$  (black line). Reprinted with permission from ref. 25.

The toolbox is based on DNA and the enzymes polymerase, exonuclease and nickase (PEN toolbox). Synthetic DNA templates

are triggered by short ssDNA strands acting as regulating signals on the production of an output signal. Activation of templates



by these ssDNA signals enables DNA polymerase to extend the oligomer-template pair resulting in fully hybridised dsDNA. Subsequently, these dsDNAs are nicked resulting in double-stranded complexes (Fig. 6E). Because these reactions are performed at a temperature close to the melting temperature of the partial duplexes, the input and output ssDNAs dissociate from their templates. Templates are inhibited by ssDNA strands that are complementary to part of the template's sequence, lack a nickase recognition site and possess a two-base mismatch at their 3' ends which prevents extension of the partial duplexes, rendering the template strands inactive. Signal and inhibition strands are degraded over time by exonuclease from which the template strands are protected by phosphorothioate modifications at their 5' ends. Fig. 6F shows the six templates that comprise the toggle switch. Two templates,  $\alpha\text{to}\alpha$  and  $\beta\text{to}\beta$  autocatalytically produce ssDNA species  $\alpha$  and  $\beta$  while templates  $\alpha\text{to}\beta$  and  $\beta\text{to}\alpha$  produce inhibitors upon activation by  $\alpha$  and  $\beta$  respectively. These four templates comprise the bistable core (Fig. 6G). Positive feedback is necessary in this system as reciprocal inhibition alone does not provide the ultrasensitive response necessary for bistability. To independently switch the system between the  $\alpha$  and  $\beta$  state two additional templates, *i.e.*  $\gamma\text{to}\alpha$  and  $\delta\text{to}\beta$  were employed (Fig. 6F and G). The authors computationally predicted switching to the  $\beta$  state by addition of single-stranded  $\delta$  and switching to the  $\alpha$  state by addition of single-stranded  $\gamma$  (Fig. 6H) and verified this bistable behaviour of the circuit experimentally (Fig. 6I). The circuit could be switched two consecutive times in a single experiment after which resources were depleted and the concentrations of templates became too low, leading to loss of functionality of the switch. Finally, the authors presented the construction of a push–push memory circuit that responds to a single input that switches the state of the bistable core. Due to the size of the circuit (eight template strands), the reaction times of the push–push circuit are large and the circuit could only be switched once. Nonetheless, the size of the circuit is comparable to *in vivo* complexity of eight genes, which is amongst the largest realisations of synthetic genetic regulatory networks performed in cells. Moreover, the systematic engineering of the push–push circuit further demonstrates the modularity of the PEN toolbox. To even further predict *in silico* the dynamical behaviour of *in vitro* PEN-based reaction networks, de Greef and colleagues,<sup>26</sup> developed an automated approach in which PEN-based networks of arbitrary complexity were screened for target temporal behaviour. Additionally, the authors reported software that optimises the template sequences for which the biochemical network robustly shows the desired non-equilibrium behaviour, narrowing the gap between *in silico* prediction and *in vitro* realisation of PEN-based circuits. The researchers verified their method by applying it to the previously described enzymatic DNA-based oscillator (*vide infra*) and used it to design a PEN-based adaptive BRN *in silico*.

As explicitly pointed out in the previous section, oscillations are a canonical example of out-of-equilibrium behaviour. Recently, several *in vitro* biochemical circuits exhibiting oscillations have been reported. Here, we highlight several pioneering studies in which oscillatory dynamics have been engineered in enzymatically driven networks, DNA circuits and *in vitro*

transcription–translation-based systems, both under batch conditions and in open reactors. Examples of oscillating BRNs that function under batch conditions include cell-free *in vitro* biochemical oscillators based on the genelet toolbox (Fig. 7A) and the PEN toolbox (Fig. 7B).

Kim and Winfree constructed an oscillator using the genelet toolbox, which consists of two synthetic DNA templates that comprise a delayed negative feedback loop.<sup>27</sup> Two genelets, regulated by RNA activator  $rA_1$  and RNA inhibitor  $rI_2$  transcribed from genelet templates  $Sw_{12}$  and  $Sw_{21}$  respectively, govern the oscillatory behaviour. The circuit could show up to five complete cycles. The researchers then added a positive feedback loop with the use of a third genelet that modulated and extended the oscillatory regime and, importantly, demonstrated the modularity of this system. To further explore the modularity and resilience of the system, Murray, Simmel and co-workers<sup>28</sup> coupled the transcriptional oscillator to several downstream loads including a DNA-based nanomechanical device and the production of a functional RNA molecule (Fig. 7A). The coupling of dynamic networks to downstream loads affects the dynamics of the original system, a process which is known as retroactivity and should be minimised. Different mechanisms were employed to couple the oscillator to several downstream processes, and for each mechanism the impact of the load on the performance of the upstream 'core oscillator' was assessed on key characteristics such as the frequency and amplitude of the oscillatory response. Reduction of retroactivity and efficient activation of the downstream reaction circuit was achieved when the coupled process was driven by appropriately fast kinetics in combination with a high-amplitude oscillatory signal. The authors achieved near zero retroactivity with the introduction of a genelet module that functions as an insulator. The insulator is activated by DNA strand  $A_2$  and inhibited by RNA strand  $rI_2$ , which are utilised and produced by the core oscillator, respectively (Fig. 7A). The insulator acts as an amplifier because small increases in the active genelet (only mildly affecting the core oscillator) drive transcription of large amounts of RNA transcript InsOut that drives the opening of a DNA tweezer. Degradation of InsOut occurs fast enough for the tweezer to follow the oscillations of the core BRN by periodically opening and closing. Therefore, the insulator module not only demonstrates the modularity of the genelet toolbox but also greatly improves the utility of *in vitro* BRNs as insulation of the core circuit allows these networks to be utilised to drive functional downstream processes, for example in DNA-based diagnostics.

In an additional study, Simmel and co-workers compartmentalised the *in vitro* transcriptional oscillator into microdroplets to study the effect of micro-scale encapsulation on *in vitro* biochemical reaction networks with complex, far-from-equilibrium dynamical behaviour.<sup>29</sup> Contrary to the study on compartmentalised BZ droplets,<sup>17</sup> biochemical reactions occur at low concentrations and, hence, show fluctuations and variability reflected by stochastic kinetics. To study these effects, the robustness of the *in vitro* transcriptional oscillator was assessed at low concentrations by measuring large populations of microdroplets simultaneously. In contrast to the work of Epstein,<sup>17</sup> synchronisation among compartmentalised oscillators did not



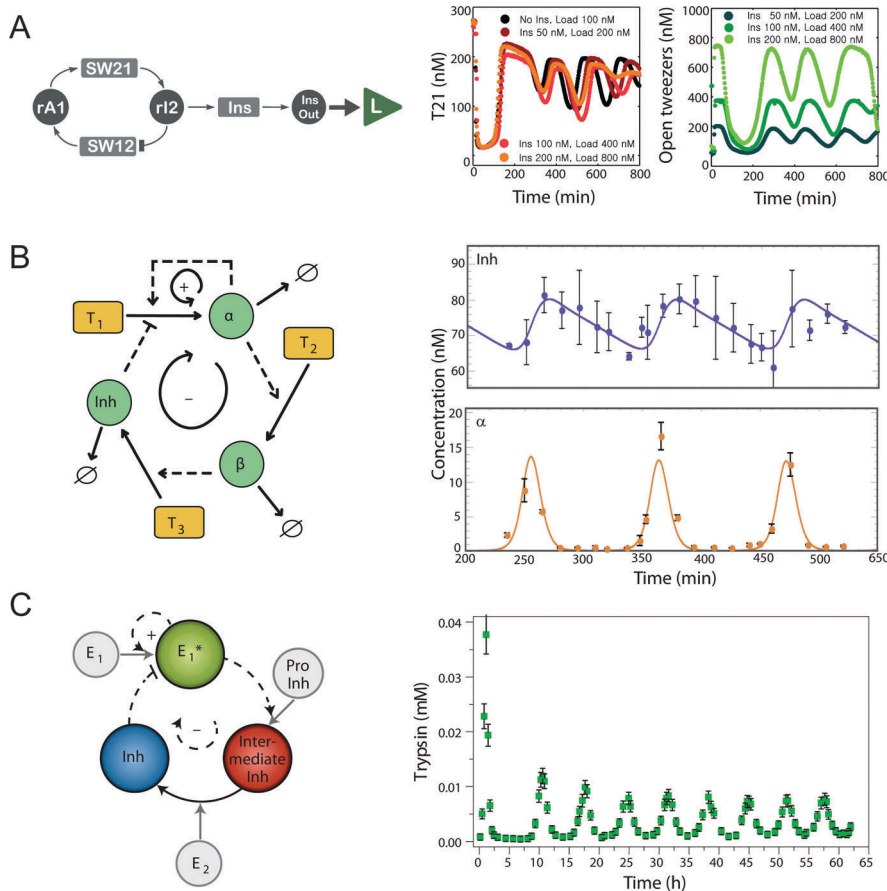


**Fig. 7** Oscillatory networks designed *de novo*. (A) Schematic representation of a genelet oscillator coupled downstream to a load via an insulator module (left). Experimental traces of the transcriptional oscillator coupled to the downstream process shows the insensitivity of the system towards the load for various insulator and DNA tweezer concentrations. Reprinted with permission from ref. 28. (B) Schematic representation of the PEN-based oscillator, including autocatalysis, activation, inhibition and degradation of primers and single-stranded DNA strands (left). The oscillatory traces of single-stranded species from experiments (dots) are shown on the right and can be fully described by a computational model (line). Reprinted with permission from ref. 30 Copyright 2011 © The authors. (C) Schematic representation of the trypsin-based enzymatic oscillator (left). Experimental traces show sustained oscillations in the concentration of trypsin for approximately 65 hours. Reprinted from ref. 32.

occur due to a lack of controlled communication between droplets, resulting in dynamical diversity of oscillatory behaviour among droplets in terms of amplitude, frequency and damping. Based on results of deterministic and stochastic models the researchers concluded that the dynamical diversity in oscillatory behaviour could be attributed to the statistical variation of reactant concentrations as a result of partitioning the system into droplets, rather than reflecting the intrinsic stochastic kinetics of the chemical reaction network itself. This extrinsic noise as a result of statistical variations during encapsulation of biochemical components is an important parameter when engineering artificial cells with preprogrammed temporal dynamics.

A PEN toolbox-based oscillator was constructed by Rondelez and co-workers (Fig. 7B),<sup>30</sup> in an analogous manner as described for their bistable switch. The network topology consists of autocatalytic synthesis of primer  $\alpha$  which activates synthesis of primer  $\beta$  which in turn serves as a primer for the production of inhibitor *inh*. Delayed inhibition of the autocatalytic synthesis of primer  $\alpha$  results from the reversible sequestration of oligomer *inh* to  $T_1$ . Highlighting the versatility of the methodology, the same group

designed an *in vitro* enzymatic DNA-based network that emulated the complex dynamics of ecological systems,<sup>31</sup> including predator-prey oscillations, competition-induced chaos, and symbiotic synchronisation.

Several groups have successfully engineered oscillating BRNs in open chemostats. Huck *et al.*<sup>32</sup> constructed a trypsin-based enzymatic oscillator under flow conditions and provided a modular approach to rationally design dissipative, tuneable and robust chemical networks. The methodology is based on translation of a basic network topology known to generate oscillations, *i.e.* a short positive feedback loop in combination with a delayed negative feedback mechanism. Positive feedback is implemented by autocatalytic production of trypsin ( $E_1^*$ , Fig. 7C) from trypsinogen ( $E_1$ ), while delayed inhibition is realised by a masked inhibitor that is converted into a fully active inhibitor by an enzymatic cascade based on trypsin and aminopeptidase. As the two enzymes that make up the negative feedback loop show a high selectivity towards their substrates, the rate of each step could be independently tuned. Using mathematical modelling, the correct balance between production and



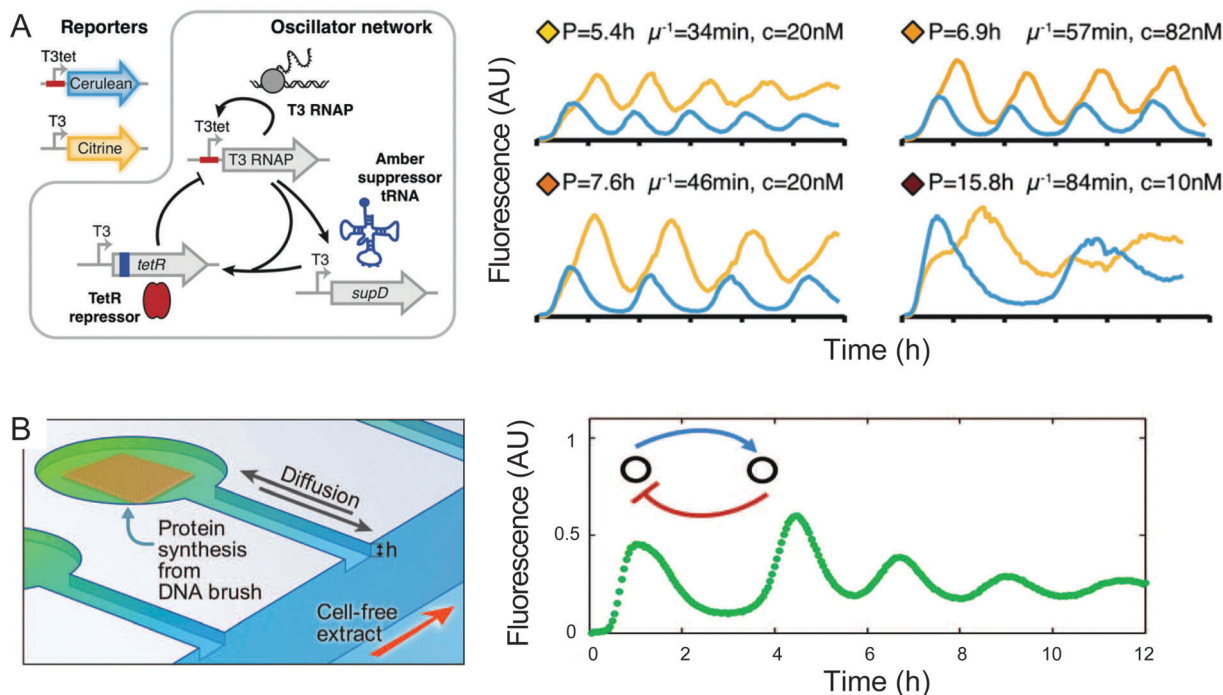


**Fig. 8** *In vitro* oscillators based on transcription and translation chemistry. (A) Operation scheme of the genetic oscillator consisting of an autocatalytic loop and delayed inhibition (left). The dynamic state of the system is measured using Cerulean and Citrine which are produced in parallel to T3RNAP and *TetR* repressor respectively. Oscillatory traces of Cerulean and Citrine show varying profiles and periods ( $P$ ) at different *supD* gene concentrations ( $c$ ) and different residence times ( $\mu^{-1}$ ) (right). Reprinted with permission from ref. 33. (B) Left: Design of the microfluidic chip in which DNA brushes are assembled in circular compartments and are connected through a capillary to a feed channel. Activator–repressor genetic networks are assembled with sigma factor for activation and the lambda phage  $\text{cI}$  for repression. Right: GFP profile of oscillatory gene dynamics in an activator–repressor network measured in the compartment. Reprinted with permission from ref. 34 Copyright 2014 © American Association for the Advancement of Science.

inactivation of trypsin necessary for sustained oscillatory behaviour was established resulting in sustained oscillations in the experimental concentration of trypsin for a wide range of flow rates. Furthermore, the authors show signal modulation by coupling of two biochemical networks each in a separate fluidic reactor, and by coupling of the out-of-equilibrium enzymatic network to complex coacervates.

*In vitro* transcription and translation chemistry (TxTl) allows the engineering of biomolecular circuits based on transfer of information between genes. Because the transcription and translation rates of *in vitro* TxTl systems decrease in time under batch conditions, experiments need to be conducted in a continuous flow setup allowing constant steady-state transcription and translation rate by exchange of reagents. Maerkl *et al.* constructed and implemented a genetic oscillator using pneumatically controlled microfluidic reactors with volumes in the nanoliter regime.<sup>33</sup> Importantly, the genetic oscillator was subjected to continuous flow allowing exchange of reagents and forcing the system out-of-equilibrium resulting in sustained oscillations for extended periods of time (Fig. 8A). The circuit design combines a short range positive feedback loop with delayed repression. The positive feedback loop is based on an autogene consisting of a gene encoding for T3 RNA polymerase and its cognate T3 promoter. Inhibition of the autogene is achieved by production of TetR repressor which binds to TetR operator sites on the T3 promoter of the autogene. Because production of TetR

repressor has to be delayed to achieve sustained oscillations, the authors introduced an Amber stop codon in the *tetR* gene resulting in premature termination of *tetR* mRNA translation. The translation rate can be increased by production of Amber suppressor tRNA which is in turn under control of the T3 autogene. Inspection of the phase diagram of the *in vitro* TxTl oscillator with respect to the *supD* DNA template concentrations and the dilution rate reveals that oscillations are observed for almost all concentrations of *supD* template. Furthermore, it reveals a decrease in the oscillation period with increasing dilution rate with oscillatory behaviour generally being established at high dilution rates.

Showing the generality of *in vitro* TxTl systems as a tool to engineer programmable molecular circuits, Bar-Ziv, Noireaux and colleagues assembled artificial cells based on two-dimensional compartments containing DNA-brushes. Programmable protein synthesis is achieved by diffusion of *Escherichia coli* cell extract through thin capillaries that connect the compartments to a central feeding channel (Fig. 8B).<sup>34</sup> Oscillatory dynamics of the genetic network is accomplished by a mixed DNA-brush encoding for an activator–repressor gene network in each compartment. The temporal period in the activator concentration scaled linearly with the length of the capillary channel, demonstrating the effect of diffusion and compartment geometry on oscillatory dynamics under non-stirred conditions. Moreover, by separating DNA-brushes encoding activator and repressor proteins into two connected



compartments, the researchers demonstrated diffusion-based information transfer resulting in a spatiotemporal pulse with a period that scales linearly with the distance between the respective compartments. The above studies illustrate enzymatic and nucleic acid-based reaction networks that display complex high-order temporal functionalities, including switching and oscillations, using a minimal set of components. Clearly, *in vitro* synthetic biologists are capable of emulating temporal life-like out-of-equilibrium dynamics using a relatively small number of biomolecular components.

## 4. Spatially extended biochemical reaction networks

In the previous section, several enzymatic BRNs that display emergent temporal functionalities, such as oscillations and bistability were discussed. While the displayed out-of-equilibrium behaviour under well-stirred conditions has provided key insights into the fundamental design principles behind their function, the coupling of reactions with diffusion in spatially extended systems is essential to understand the complex spatial ordering and dynamic behaviour of the intra- and intercellular environment. Indeed, reaction–diffusion mechanisms are responsible for a wide range of important regulatory functions *in vivo*, such as neuron polarisation, spatial organisation during mitosis and morphogenesis.<sup>6,7</sup>

In this section, we discuss *in vitro* biochemical model systems that display higher-order spatiotemporal behaviour when subjected to spatially extended or spatially modulated conditions. Herein, we mainly consider enzymatic systems, where positive or negative feedback is introduced *via* autocatalysis or inhibition. We also highlight the use of molecular programs based on nucleic acids to generate spatial patterns.

Many of these phenomena can be modelled and understood with simple sets of differential equations, often using a Michaelis–Menten description of the reaction kinetics. For example, the well-known FitzHugh–Nagumo model was developed as a model for neuron excitability, and is now used to study a wide range of biochemical reaction–diffusion systems. In fact, by combining these systems with accurate kinetic models, they can also be utilised to estimate physicochemical parameters of biochemical reactions, as demonstrated elegantly by Grzybowski and co-workers.<sup>35</sup> Using micropatterned agarose stamps to introduce freely-diffusing enzymes into a polyacrylamide hydrogel containing immobilised ligands, the authors were able to estimate protein–ligand dissociation constants down to the picomolar range by fitting the experimental reaction–diffusion patterns to computational models. To engineer higher-order spatial behaviour in enzymatic reaction networks, feedback is required and, in the simplest case, can be generated by an intrinsic property of the enzyme itself. Taylor and co-workers<sup>36</sup> investigated the urea–urease reaction, in which urease catalyses the conversion of urea to CO<sub>2</sub> under production of base, NH<sub>3</sub>. Because the enzyme–substrate complex exists in an active protonated form and an inactive biprotonated form, a bell-shaped rate–pH dependence arises with a maximal reaction rate

at pH 7. Therefore, if the initial pH of the base-producing reaction is adjusted to a pH below 7, the reaction accelerates as it progresses. This autocatalytic behaviour was first investigated in a continuously stirred tank reactor (CSTR), in which a solution of urea and urease produced a sharp switch from pH 3 to pH 9 after an induction period of approximately 1000 s. Next, a quasi-two-dimensional setup was constructed and a propagating pH front with constant velocity could be observed after initiation of the system (Fig. 9A). Both the front velocity and the number of spontaneous initiations increased at higher urease concentrations. Simulations, assuming Michaelis–Menten kinetics and including substrate and product inhibition, could reproduce the experimental observations and showed that the diffusion of basic products drives front propagation, while the sharpness of the front is maintained throughout the reaction (Fig. 9B).

A related single-enzyme system was explored by Epstein and co-workers,<sup>37</sup> who employed the ping-pong mechanism of glucose oxidase as a source of autocatalysis. Glucose oxidase (GOx) in oxidised form catalyses the oxidation of glucose to glucono- $\delta$ -lactone, while the reduced form of GOx reduces ferricyanide to ferrocyanide, producing two protons and returning to its original oxidised state. Because the GOx catalytic rate constant is pH-dependent and protons are produced, the overall enzymatic reaction displays autocatalysis, as evident by an accelerating decrease in pH from pH 7 to 3 as the reaction progresses. Similar to the work of Taylor and colleagues,<sup>36</sup> a propagating pH front with constant velocity develops in thin slabs of polyacrylamide gel, both in a quasi-1D setup and a quasi-2D continuously fed unstirred reactor (Fig. 9C).

Subsequently, negative feedback was introduced using H<sub>2</sub>O<sub>2</sub>, which restores the enzymatically reduced ferrocyanide into ferricyanide, raising the pH and giving rise to a propagating pulse with constant velocity (Fig. 9C). Both experimentally and by simulations, it was shown that tuning the H<sub>2</sub>O<sub>2</sub> concentration, led to either spatial bistability or excitability in the form of a propagating pulse. Importantly, kinetic simulations revealed that the velocity of the wave front is proportional to the square root of both the substrate and enzyme concentration. This relationship is often encountered in the general theory of chemical waves and is known as the Fisher–Kolmogorov relation. Because the urea–urease reaction and the GOx system involve only a single enzyme and an intrinsic feedback mechanism, they represent some of the simplest enzymatic systems capable of spatial pattern formation, such as propagating waves and pulses in an unstirred reactor. This simplicity can be used in a bottom-up fashion to understand the fundamental mechanisms behind higher-order behaviour observed in complex natural systems.

A more advanced system was reported by the group of Schille,<sup>38</sup> who investigated the *in vitro* behaviour of the Min protein system, responsible for determining the position of the division septum at the centre of bacterial cells during mitosis. The adenosine triphosphatase MinD binds to a lipid membrane as a dimer, while MinE forms a complex with MinD to induce ATP hydrolysis, releasing both enzymes from the membrane. *In vivo*, a MinD patch forms at one of the cell's poles, while MinE forms a



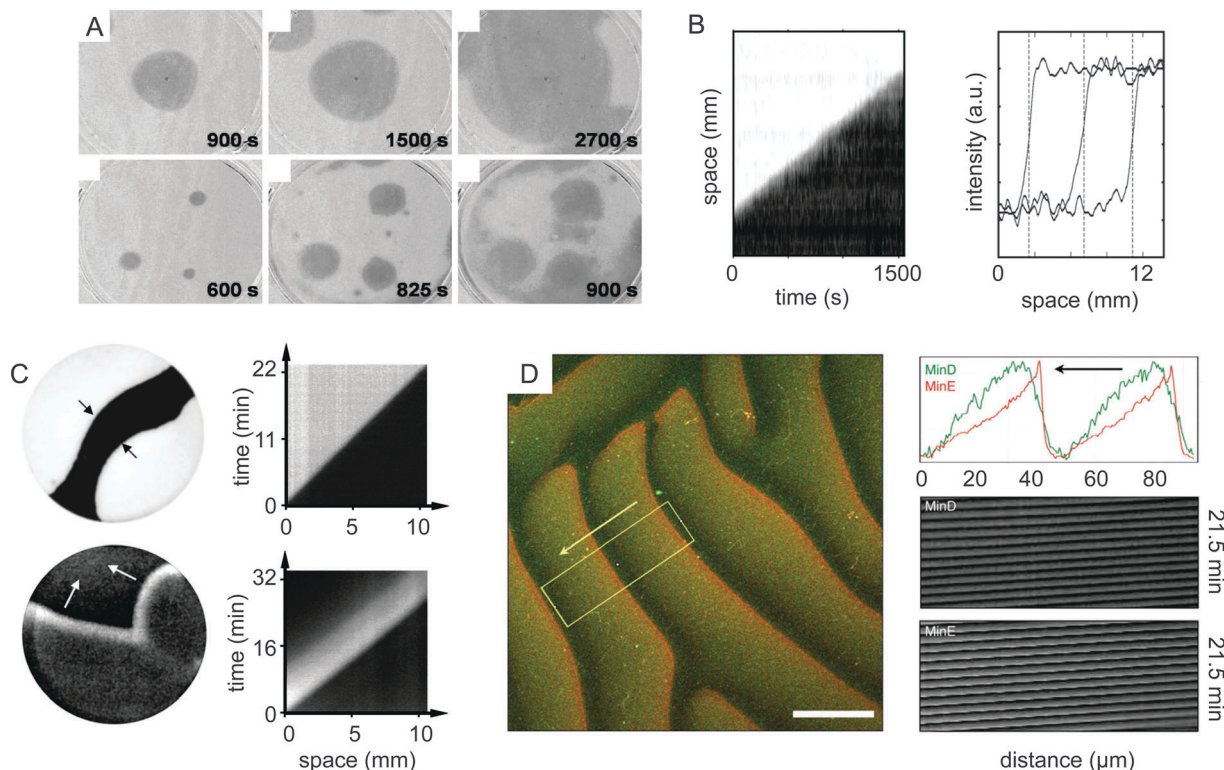


**Fig. 9** Spatiotemporal patterns in enzymatic systems. (A) Propagating pH waves of constant velocity in the urea-urease reaction. Waves travel radially outwards and are visualised using pH indicator cresol red at high (dark) and low (light) pH. (B) Kymograph and intensity-space plots showing constant velocity and front sharpness. Reprinted with permission from ref. 36 Copyright 2012 © Elsevier. (C) Propagating pH fronts (top) and pulses (bottom) in the glucose oxidase reaction using a quasi-2D setup (left). Corresponding kymographs displaying constant velocity of the wave front and pulse, respectively (right). Colours correspond to presence of ferrocyanide (dark) and ferricyanide (light). Reprinted with permission from ref. 37 Copyright 2007 © National Academy of Sciences, U.S.A. (D) Confocal fluorescent images of surface waves caused by MinD and MinE, labeled with BODIPY (green) and Alexa647 (orange) fluorophores, respectively. Graph depicts intensity profile in the area indicated in the image, while kymographs show constant velocity and wavelength of propagating waves. Reprinted with permission from ref. 38 Copyright 2008 © American Association for the Advancement of Science.

ring around the MinD patch, leading to disassembly of MinD and reassembly of a new patch at the other cell pole. This oscillating behaviour results in a time-averaged concentration minimum of MinD in the middle of the cell. The distribution of a third enzyme MinC directly maps onto the MinD pattern and inhibits the membrane attachment of FtsZ, whose polymerisation is responsible for the initiation of division septum formation at the bacterial cell poles. The authors reconstituted purified MinD and MinE with ATP *in vitro* in the presence of a supported lipid bilayer and observed spontaneous symmetry breaking and initiation of oscillating waves of constant velocity on the lipid surface (Fig. 9D). The average front velocity increased while the average wavelength decreased upon increasing MinE concentration, similar to the studies discussed above.<sup>36,37</sup> Importantly, confocal images of the spatial patterns of fluorescently-labeled MinD and MinE revealed a small lag between the sharp trailing edge of MinD and the trailing edge of MinE (Fig. 9D). Similar to *in vivo* observations, this indicates MinE complexation with MinD, followed by subsequent release of the complex from the membrane. MinD then reassembles onto the membrane behind the trailing edge, resulting in the build-up of shallow MinD and MinE gradients as leading edges of the next oscillation.

To understand the mechanism by which the surface waves are generated, a simple reaction-diffusion model was used which could qualitatively reproduce the shape of the surface waves by taking into account cooperative effects during MinD and MinE binding. However, the wavelength and the sawtooth-like appearance of – and the phase difference between – MinD and MinE waveforms could not be well reproduced. Meanwhile, theoretical studies have provided a more accurate mechanism that is based on the polymerisation of MinD–MinE heterotetramers.<sup>39</sup> Nonetheless, the approach elegantly shows the application of a relatively simple, dissipative two-enzyme system *in vitro*, displaying complex spatiotemporal behaviour that resembles the *in vivo* situation.

The previous studies illustrate how simple enzymatic systems containing few components can display various higher-order functionalities when starting from homogeneous initial conditions. However, cells are often exposed to time-varying signals, such as gradients and oscillations, and spatial patterns. The modulation of a spatiotemporal input signal to produce a relevant intracellular output is an important feature cells use to sense and accordingly react to their environment. This is for example apparent in the ultrasensitive or switch-like response to chemical gradients in chemotaxis or signal transduction pathways.



Huck, de Greef and co-workers<sup>40</sup> investigated the possibility of spatial modulation using a bottom-up strategy, starting with a simple one-enzyme system consisting of the protease  $\beta$ -trypsin, a fluorogenic substrate that becomes fluorescent upon cleavage, and a strong, reversible inhibitor. Similar to the work of Grzybowski *et al.*,<sup>35</sup> fluorogenic substrate and inhibitor were immobilised in a polyacrylamide hydrogel, while freely-diffusing trypsin was introduced using micropatterned agarose stamps (Fig. 10A). The immobilisation of the fluorogenic substrate is important because it allows the direct read-out of trypsin activity in the hydrogel. In the absence of inhibitor, trypsin propagates through the hydrogel *via* diffusion and generates a broad product front which overlaps with the propagating trypsin front. Upon addition of a strong, reversible inhibitor the system displays ultrasensitivity by spatially extended molecular titration. The molecular titration effect is based on the fact that the inhibitor binds more strongly to the enzyme compared to its substrate resulting in sequestration of enzyme activity until the total enzyme concentration surpasses the inhibitor concentration. This results in a sharp increase in product conversion and as a result, the spatial propagation of enzyme activity is modulated, significantly sharpening the product front (Fig. 10B). A system of partial differential equations, taking into account enzymatic activity, inhibition and diffusion of the reaction components, was solved on a representative two-dimensional geometry (Fig. 10B). The simulations corresponded well with the experimental data and revealed how the steepness of product fronts relates to the concentration and diffusion constant of the inhibitor.

A similar approach was explored by Mrksich and colleagues,<sup>41</sup> using a system based on Abelson tyrosine kinase (Abl), which contains a catalytic domain that phosphorylates tyrosine residues and a Sarcoma homology 2 (SH2) domain that binds the phosphorylated substrate. Due to local proximity effects as a result of binding of the SH2 domain to the product, the enzymatic reaction proceeds autocatalytically on a self-assembled monolayer (SAM)

consisting of immobilised peptide substrates (Fig. 11A). By patterning the SAM with regions of substrate peptide and product phosphopeptide followed by exposing the surface to a uniform solution of Abl kinase and ATP, the reaction spatially propagates towards regions of unreacted substrate. Subsequently, patterns with different boundary-to-surface ratios were fabricated and the space-averaged initial reaction rate was measured. The authors concluded that the overall rate increases upon increasing the boundary-to-surface ratio as the reaction proceeds most rapidly on the interface between surface-bound substrate and product (Fig. 11B).

In the previous study, an enzymatic reaction-diffusion system was coupled to the specific organisation of reaction components on the surface thereby controlling the spatial distribution of biochemical output. Similarly, Huck and colleagues<sup>42</sup> combined enzymatic autocatalysis and molecular titration to develop a system which is able to sense the spatial distribution of enzymes. Extending the work by de Greef & Huck *et al.* (*vide supra*),<sup>40</sup> positive feedback was added to the trypsin-inhibitor system by employing trypsinogen, a zymogen that is autocatalytically cleaved into trypsin. A biochemical analog-to-digital converter was engineered by introducing trypsin *via* a micropatterned agarose stamp to a polyacrylamide gel containing immobilized fluorogenic substrate and freely-diffusing trypsinogen and inhibitor (Fig. 11C). Depending on the width of the embossed pillars, the trypsin diffusion front either adopts a radial or one-dimensional character. For narrow pillars, diffusion of trypsin into the gel occurs from a point-source and the inhibitor can completely suppress the autocatalytic activation of trypsinogen. In contrast, wider pillars generate a one-dimensional diffusion front with a smaller boundary-to-surface ratio resulting in a failure of the inhibitor to inactivate trypsin, thus inducing a traveling wave of trypsin activity throughout the gel (Fig. 11C). This experiment exhibits threshold sensing, *i.e.* the combination of analog input signals (trypsin concentration, pillar width and diffusion time) is transformed into a digital output, *i.e.* propagation

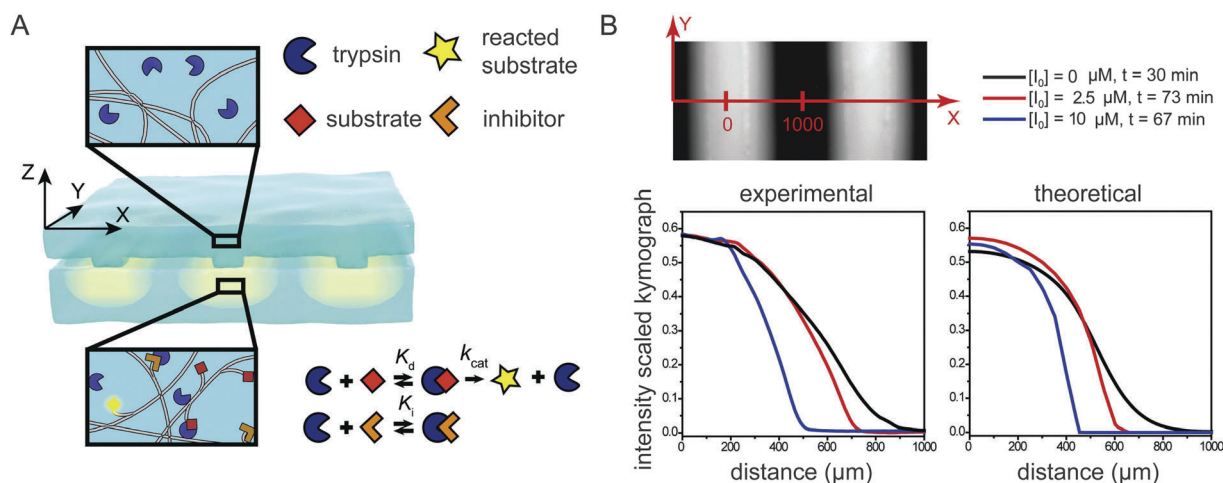
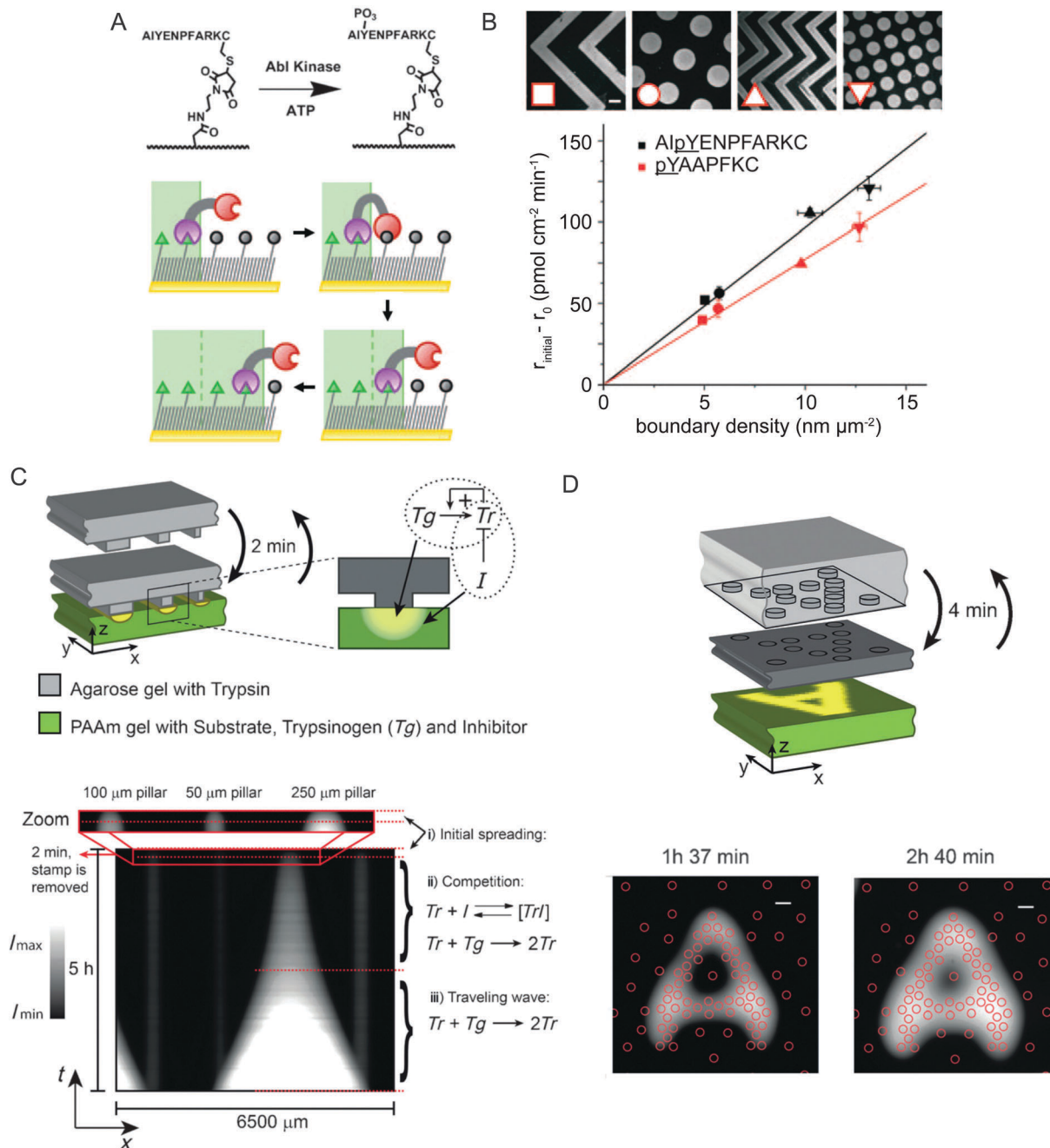


Fig. 10 Ultrasensitivity through molecular titration using a strong, reversible inhibitor. (A) Experimental setup of wet stamping experiments. (B) Intensity profiles in the polyacrylamide gel at various inhibitor concentrations, in experiments (left) and simulations (right). Reproduced with permission from ref. 40 Copyright 2013 © Elsevier.





**Fig. 11** Spatial modulation in *in vitro* biochemical reaction networks. (A) Reaction scheme and mechanism of a spatially propagating reaction based on Abl kinase with product-binding SH2 domain. (B) The average initial reaction rate ( $r_{\text{initial}}$ , corrected for the background rate  $r_0$ ) for patterns with different boundary densities, for a high-affinity peptide (black curve) and a low-affinity peptide (red curve). Reproduced with permission from ref. 41 Copyright 2011 © Wiley-VCH Verlag GmbH & Co. KGaA. (C) Schematic setup of the analog-to-digital wet stamping experiment, with kymographs showing the evolution of fluorescent product conversion for different pillar widths. (D) Schematic setup of the pattern recognition experiment and fluorescent micrographs of product conversion. The position of pillars in the agarose stamp is shown in red. Reproduced with permission from ref. 42 Copyright 2014 © Wiley-VCH Verlag GmbH & Co. KGaA.

or complete inhibition of enzyme activity depending on a threshold level of the input. Next, the authors extended the system with a second polyacrylamide gel layer that only contains freely-diffusing trypsinogen and inhibitor and demonstrated that such a system is capable of responding to the density of pillars on the agarose stamp (Fig. 11D).

Isalan and co-workers<sup>43</sup> demonstrated the power of *in vitro* synthetic biology by engineering a minimal biochemical system capable of generating expression patterns analogous to the complex gene system responsible for *Drosophila* embryonic development. Spatiotemporal control over gene activity is essential for embryonic development and involves concentration gradients



of a large number of morphogens that activate or repress transcriptional and translational activity. Specifically, the Bicoid morphogen determines the anterior–posterior orientation of the embryo through spatial concentration gradients from the cell's pole and affects members of the gap gene system in a concentration-dependent manner to induce pattern-formation. In the experimental setup, magnets were used to spatially localise paramagnetic beads coated with the DNA of three genes A, B and C, encoding for zinc finger-based transcription repressor proteins (Fig. 12A–C). Gene A represses gene B and C and is located at the edges of the reaction chamber, while gene B (repressing gene C) and gene C are present ubiquitously in the setup. T7 polymerase activates expression of gene A and B and is injected at the edges of the chamber to generate a spatial concentration gradient, emulating the function of Bicoid. Finally, Gene C is activated by homogeneously distributed SP6 polymerase that serves as a nonexplicit model for other interactions in the gap gene system (Fig. 12A). As a result, patterns of expression levels are formed in the reaction chamber (Fig. 12D). Gene A and B are both activated by T7 polymerase at the chamber edges and therefore display low

expression levels in the chamber's centre. Because gene B is repressed by protein A, the expression of protein B at the edges is suppressed. Expression of protein C is exclusively seen in the middle of the chamber, due to repression by proteins A and B. Although significantly simplified, this system shows that complex natural behaviour such as transcriptional pattern-formation can arise in a rationally designed *in vitro* system constructed from minimal components.

The above studies clearly illustrate how simple enzymatic reaction networks are combined with spatial patterning or delivery of reaction components to modulate spatiotemporal input patterns. However, modularity and programmability of these networks is generally low, because the rational redesign of enzymes can be extremely challenging. In contrast, synthetic nucleic acids such as DNA and RNA are easily programmable, allowing rational design of sequence, length and interactions. As a result, tuning of reaction parameters such as rate constants, diffusion coefficients and network connectivity over several orders of magnitude is relatively straightforward. Similar to enzymatic reaction networks, coupling of reaction to diffusion

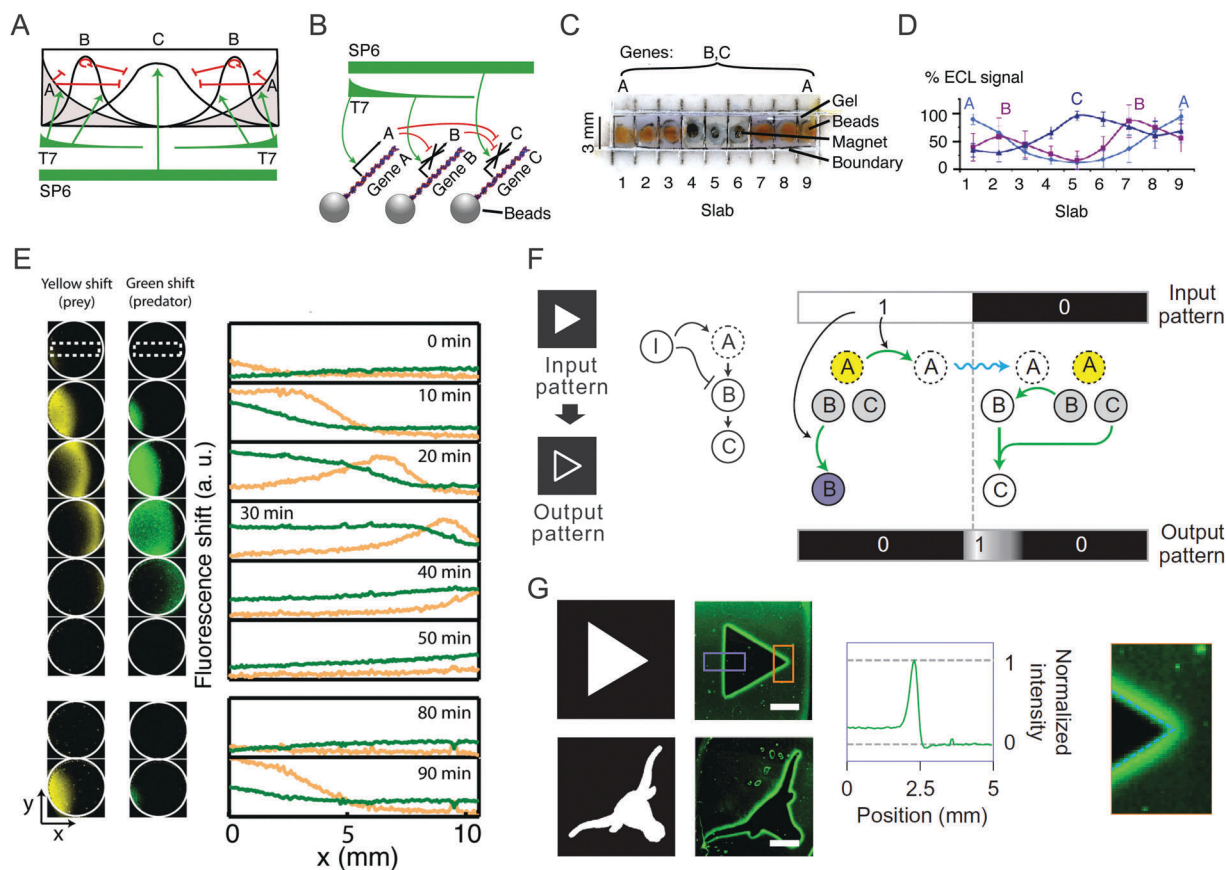


**Fig. 12** Spatial patterns in biochemical reaction networks involving nucleic acids. (A) Schematic overview of network interactions mimicking embryonic expression patterns in *Drosophila*. (B) Schematic overview of the implementation of the artificial reaction network. (C) Compartmentalised experimental setup. (D) Normalised expression levels measured by enhanced chemiluminescence (ECL) from Western blots, data of four replicate experiments plus one standard deviation. Reproduced with permission from ref. 43 Copyright 2005 © The authors. (E) Fluorescent images of DNA-based predator–prey waves (green and yellow, respectively) and corresponding profiles in the region indicated by the dashed rectangle. Reproduced with permission from ref. 45 Copyright 2013 © American Chemical Society. (F) Principle of edge detection via a DNA-based incoherent feed-forward loop. Colours indicate caged (yellow), inactive (grey), ablated (purple) and active (white) species. (G) Fluorescent images showing edge detection after selective UV illumination. Scale bars, 3 mm. Reproduced with permission from ref. 46 Copyright 2013 © Macmillan Publishers Ltd.



in spatially extended systems based on nucleic acids can lead to important insights into the complex spatiotemporal ordering in living systems. An early example is the work of McCaskill and Bauer<sup>44</sup> who, in their study on *in vitro* evolution, used the Q $\beta$  replicase enzyme to amplify short RNA strands in a long thin capillary. Because Q $\beta$  replicase can use both the plus and minus strand of a double-stranded RNA as a template, replication occurs autocatalytically and traveling concentration waves of constant velocity were observed.

More recently, Estévez-Torres, Rondelez and colleagues<sup>45</sup> employed the PEN toolbox to engineer a reaction network *de novo* displaying predator–prey oscillations in a quasi-two-dimensional closed reactor. Predator–prey dynamics are classically described by Lotka–Volterra type reaction–diffusion equations and involve prey growth by consuming food and predator growth by consuming prey, leading to oscillatory spatiotemporal behaviour. In this study, prey growth was implemented by a template species (*i.e.* the ‘food’) onto which prey can hybridise. Subsequently, two copies of prey are released after extension and nicking. Prey can bind to predator species, after which polymerase turns the prey into a predator. Finally, exonucleases degrade both prey and predator into unreactive products. When the three DNA fragments and three enzymes are homogeneously distributed in a spatially extended reactor, traveling waves of predator chasing prey were observed (Fig. 12E). One-dimensional reaction–diffusion models agreed well with experimental data and the relation between front velocity and reaction parameters, such as the diffusion coefficient of the predator species and the concentration of polymerase, was found to obey the Fisher–Kolmogorov relation, similar to the results described above for enzymatic reaction networks.<sup>37</sup>

The programmability of synthetic DNA oligonucleotides was elegantly utilised by Ellington, Chen and co-workers,<sup>46</sup> who engineered an enzyme-free DNA-based molecular program capable of spatial edge detection. The system is based on an incoherent feed-forward loop consisting of an input signal I, intermediate DNA species A and B and output species C. In the reaction network, input I activates A but inactivates B, while A activates B, which in turn produces active species C (Fig. 12F). A highly-crosslinked polyacrylamide hydrogel was used to limit the diffusion of chemical species and a mask was used to selectively illuminate parts of the hydrogel, serving as a spatially modulated input signal I. In illuminated regions of the hydrogel output C is not produced because B is inhibited, while in unilluminated areas C is also not produced, because A cannot activate B to produce C. Critically, near the boundary between regions species A can diffuse from light into dark regions, activating species B and subsequently producing output C (Fig. 12F). Because species C is labeled with a fluorophore, a fluorescent signal is generated only at the edges of the UV illuminated region (Fig. 12G). Furthermore, the authors show that by changing the connectivity of the network, for example by changing DNA sequences or adding new species, the behaviour of the molecular program could be tuned in a modular fashion. In this study, the bottom-up engineering of rationally designed molecular circuits is combined with spatially modulated input signals to generate truly emergent behaviour.

In the previous two sections, we have described enzymatic and nucleic acid-based reaction networks that emulate complex spatiotemporal ordering using a minimal set of components. The studies presented here demonstrate that *in vitro* synthetic biologists are capable of emulating life-like out-of-equilibrium behaviour using relatively small networks.<sup>4</sup> In the next section, we discuss emerging applications of cell-free synthetic biology.

## 5. Applications and perspective

Due to the modularity and inherent biocompatibility of engineered biomolecular circuits, applications of this technology in the biomedical sciences are within reach. We will briefly highlight several emerging applications of this technology in the areas of cell-free genetic biosensors, biological nanofactories capable of reciprocal communication with living systems, and in the area of autonomous materials.

A first emerging application comprises cell-free genetic biosensors. In contrast to genetically engineered biosensing cells, which might have limited detection ranges due to membrane impermeability of the analytes and which may be difficult to commercialise due to official regulations of genetically modified organisms, cell-free biosensors can be readily made using coupled *in vitro* transcription translation systems. Pellinen *et al.*<sup>47</sup> for instance used an *E. coli* extract to produce firefly luciferase as reporter in response to specific analytes. The authors showed that their cell-free approach allowed for improved sensitivity, wider detection range and faster assays combined with minimal preparation times. Recently, Collins *et al.*<sup>48</sup> have taken this approach to the next level by freeze drying cell-free synthetic gene networks onto paper and other porous materials (Fig. 13A). The resulting abiotic materials are sterile and stable at room temperature, allowing for facile storage and distribution. Retaining their *in vitro* transcription and translation capability, these materials can be activated at will by simply adding water. As such, the paper-based platform allows for the safe use of engineered gene networks beyond the lab, *e.g.*, in the clinic and industry, presumably at a low cost. The authors demonstrated their platform as glucose sensors and strain-specific Ebola virus sensors making use of a colorimetric output. Due to the modularity of the paper-based approach, arbitrary reaction networks from the ever growing toolbox of synthetic biology can be added resulting in paper-based biosensors for ultrasensitive multiplexed diagnostics. In addition, simple cameras present on many contemporary mobile phones can be used to quantitatively detect the optical readout. Therefore, this technique paves the way for the creation of low-cost biosensors that can be embedded ubiquitously into daily life.

A second emerging application of cell-free circuits consists of biological nanofactories that can communicate with living systems. This technology is based on the fact that cells sense and respond to their environment, and each other, using extracellular molecules. Bentley *et al.*<sup>49</sup> engineered nanofactories, *i.e.* macromolecules consisting of modules that can target, sense and synthesise molecules, to trigger communication between



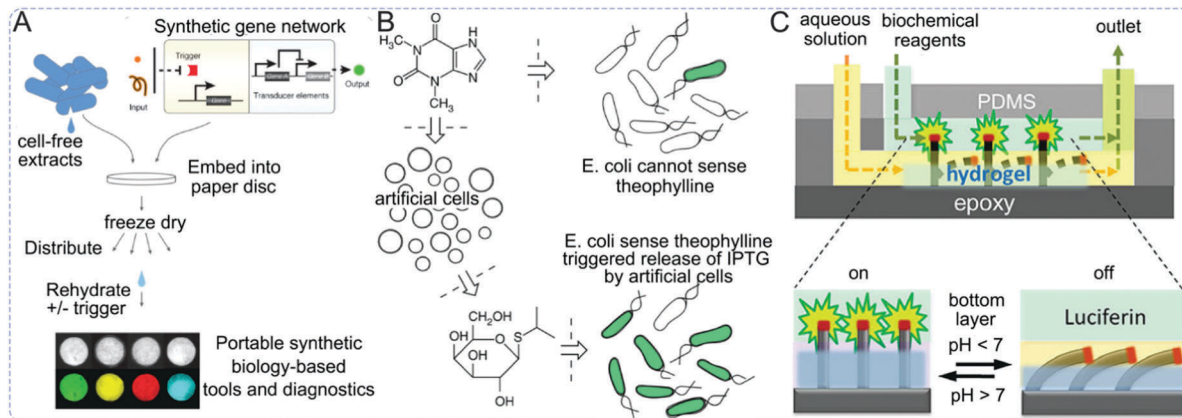


**Fig. 13** Selected emerging applications of engineered biomolecular circuits. (A) Usage of synthetic-biology-based technologies outside the laboratory is facilitated by paper-based technology where cell-free genetic networks are freeze-dried and, after distribution, reactivated by rehydration. Reprinted with permission from ref. 48 Copyright 2014 © Elsevier. (B) Engineered, artificial, non-living cellular mimics activate (or repress) natural sensory pathways in living cells through chemical communication, allowing new opportunities in controlling cellular behaviour without the use of genetically modified organisms. Reprinted with permission from ref. 50 Copyright 2014 © The authors. (C) A signal converter translating chemical signals at the nanoscale (pH changes) to macroscopic optical outputs using chemo-mechanical feedback loops. Reprinted with permission from ref. 51 Copyright 2013 © American Chemical Society.

different bacterial populations. Their design comprises an antibody to selectively target the outer-membrane of bacteria where it triggers a quorum sensing response by means of cell-surface synthesis and delivery of quorum signalling molecules.

In addition, the technology was used to trigger communication between two bacterial populations that otherwise are non-communicative. The idea of targeting existing cell signalling pathways has also been pursued by Mansy and coworkers<sup>50</sup> who engineered artificial, non-living cellular mimics to activate (or repress) existing sensory pathways of living cells through chemical communication. They expanded the senses of *E. coli* by adding liposomes containing a genetic network that converts a chemical message that *E. coli* cannot sense to a molecule that activates a natural cellular response (Fig. 13B). This approach may allow for new opportunities in engineering cellular behaviour without exploiting genetically modified organisms. Moreover, it paves the way to revolutionise the treatment of bacterial infections as molecules that interrupt or modulate bacterial communication rather than their viability exert less selective pressure to develop resistance.

Other interesting applications may also arise from the coupling of biochemical and mechanical processes. Mechano-chemical conversions are abundant in living systems, which are able to mechanically respond to a changing chemical environment. However, although being a highly desired property for next-generation materials and biosensors, mechano-chemical feedback is generally lacking in synthetic systems. Interesting in this respect is the development of Self-regulated Mechano-chemical Adaptively Reconfigurable Tunable Systems (SMARTS) by Aizenberg and coworkers.<sup>51</sup> This technology utilises catalyst-bearing microstructures embedded into a hydrogel which mechanically deforms upon a biochemical signal. In this way for instance a pH change can switch on/off an optical output producing biochemical process (Fig. 13C). The vast variety of switchable biochemical reactions in combination with the wide

variety of triggers that induce a hydrogel response (ranging from pH, glucose or other metabolic compounds, light to temperature) and the range of possible outputs (*i.e.* fluorescence, gas generation, visible colour change) paves the way for a new generation of bio-responsive materials and biosensors that can autonomously function in and on the human body.

In this Tutorial Review we have highlighted a diverse range of studies on chemical self-organisation starting from seminal work on the BZ reaction to more recent endeavours employing biological components. It has now become clear that chemistry is moving beyond the synthesis of molecules to the design and construction of chemical reaction networks. In a similar way, biochemists are shifting their attention from the characterisation of single biological molecules to understanding how these components together are able to produce meaningful biological responses. The central element of these multidisciplinary research efforts is thus to understand and emulate complex kinetic networks of regulatory circuits in the living cell. To make advances in this field will require extensive collaboration between physical chemists and biologists and a firm integration of mathematical modelling of complex reaction networks into the design process. The bottom-up construction of CRNs will give us a unique approach to understand, predict, and possibly control the behaviour of complex molecular systems.

## 6. Glossary

- Adaptation** Adaptation refers to the ability of a system to respond to a change in input stimulus and then return to its prestimulus output level, even when the change in input persists
- Autocatalysis** The process in which a reactant drives (directly or indirectly) the formation of itself



Belousov–Zhabotinsky (BZ) reaction	A homogeneous, oscillating chemical system based on inorganic chemistry involving bromous acid, bromide and a metal-ion catalyst	Spatially-extended	A spatially-extended molecular system can be followed in space, <i>e.g.</i> propagating pulses or a wave train
Bistability	A system exhibits bistability when it is able to exist in two different stable temporal steady states	Stimuli-responsive	The ability of a system to respond to an external input which can be chemical, mechanical or physical
Chemical self-organisation	The process by which a dissipative (bio)chemical system of several components becomes ordered in space and time	Synchronisation	The spontaneous process by which independent oscillators interact and assume the same temporal frequency
Chemo-mechanical feedback loop	Dynamic materials that are able to mechanically respond to changes in their chemical environment	Systems chemistry	Emulation of complex emergent phenomena encountered in living systems utilising a framework that is based on mostly abiotic homogeneous chemistry
Entrainment	The engineered process by which independent oscillators interact with an external load and assume the same period	Threshold sensing	Combined analog input signals that are transformed into a digital output, depending on the threshold levels of the inputs
Excitability	A system is excitable when it produces an output signal as a response to an input level above a certain threshold	Ultrasensitivity	Small changes in stimulus trigger large changes in the response, and is typically described by a sigmoidal relationship between the two.
Fold-change detection	A system which responds to fold changes in input rather than to absolute changes in input	Unstirred	The reaction solution is not mixed and, hence, driven by diffusion
Front propagation	A spike signal that emanates from a source and moves in space as time progresses	Well-stirred	Continuously or repeatedly mixing of the reaction solution in order to mix, cool, dissolve, <i>etc.</i> , any or all of the reaction components
<i>In vitro</i> synthetic biology	The engineering of new and existing life-like behaviours from the bottom up using biological components	Quorum sensing	A mechanism by which individual components of a system correlate their stimuli and responses to the local population density, by making use of signalling molecules
Incoherent feedforward loop	The incoherent feedforward topologies (IFFL) class suppresses a direct response of the output activity to a change in input with a delay. In an IFFL, the output module is subjected to two regulations both originating from the input but with opposing signs in their regulatory activity	Retroactivity	The quantity that changes the dynamics of an upstream system when its output is connected to downstream components, where upstream and downstream are defined by the direction in which the signal travels
Kymograph	A graphical representation of spatial position over time to measure motion or pressure		
Oscillations	Signals in which temporal variations about a central value occur with well-defined frequencies		
Programmed pattern formation	The intended generation of complex spatial organisations in a system		
Reaction–diffusion	Reaction–diffusion model systems explain how the concentration of molecules distributed in space changes under the influence of local (bio)chemical reactions, in which molecules are produced or consumed, and diffusion, which causes the molecules to spread out in space		
Self-replication	The trait of a dynamical system to make an identical copy of itself		
Signal transduction	A biochemical chain of events inside a cell that ensures a metabolic, genetic response		

## Acknowledgements

All authors acknowledge financial support from the Netherlands Organisation for Scientific Research (NWO): Graduate Programme 2010, VENI Grant: 722.012.0001, ECHO-STIP Grant: 717.013.001 and Gravity program 024.001.035. The authors acknowledge the ICMS Animation Studio, TU/e for production of the TOC.

## References

- 1 K. Kaneko, *Life: An Introduction to Complex Systems Biology*, Springer, Berlin, New York, 2006.
- 2 B. Hess and A. Mikhailov, *Science*, 1994, **264**, 223–224.
- 3 U. S. Bhalla and R. Iyengar, *Science*, 1999, **283**, 381–387.



- 4 U. Alon, *Nat. Rev. Genet.*, 2007, **8**, 450–461.
- 5 W. A. Lim, C. M. Lee and C. Tang, *Mol. Cell*, 2013, **49**, 202–212.
- 6 O. Brandman and T. Meyer, *Science*, 2008, **322**, 390–395.
- 7 E. Karsenti, *Nat. Rev. Mol. Cell Biol.*, 2008, **9**, 255–262.
- 8 S. Soh, M. Byrska, K. Kandere-Grzybowska and B. A. Grzybowski, *Angew. Chem., Int. Ed.*, 2010, **49**, 4170–4198.
- 9 I. R. Epstein and J. A. Pojman, *An Introduction to Nonlinear Chemical Dynamics: Oscillations, Waves, Patterns, and Chaos*, Oxford University Press, New York, 1998.
- 10 R. F. Ludlow and S. Otto, *Chem. Soc. Rev.*, 2007, **37**, 101–108.
- 11 P. Schwille and S. Diez, *Crit. Rev. Biochem. Mol. Biol.*, 2009, **44**, 223–242.
- 12 A. C. Forster and G. M. Church, *Genome Res.*, 2007, **17**, 1–6.
- 13 A. N. Zaikin and A. M. Zhabotinsky, *Nature*, 1970, **225**, 535–537.
- 14 K. J. M. Bishop and B. A. Grzybowski, *Phys. Rev. Lett.*, 2006, **97**, 128702.
- 15 Z. Noszticzius, W. Horsthemke, W. D. McCormick, H. L. Swinney and W. Y. Tam, *Nature*, 1987, **329**, 619–620.
- 16 J. Horváth, I. Szalai and P. De Kepper, *Science*, 2009, **324**, 772–775.
- 17 M. Toiya, V. K. Vanag and I. R. Epstein, *Angew. Chem., Int. Ed.*, 2008, **47**, 7753–7755.
- 18 A. F. Taylor, M. R. Tinsley, F. Wang, Z. Huang and K. Showalter, *Science*, 2009, **323**, 614–617.
- 19 O. Steinbock, P. Kettunen and K. Showalter, *J. Phys. Chem.*, 1996, **100**, 18970–18975.
- 20 A. Hjelmfelt, F. W. Schneider and J. Ross, *Science*, 1993, **260**, 335–337.
- 21 M. Nakajima, K. Imai, H. Ito, T. Nishiwaki, Y. Murayama, H. Iwasaki, T. Oyama and T. Kondo, *Science*, 2005, **308**, 414–415.
- 22 V. Noireaux, R. Bar-Ziv and A. Libchaber, *Proc. Natl. Acad. Sci. U. S. A.*, 2003, **100**, 12672–12677.
- 23 J. Kim, K. S. White and E. Winfree, *Mol. Syst. Biol.*, 2006, **2**, 68.
- 24 J. Kim, I. Khetarpal, S. Sen and R. M. Murray, *Nucleic Acids Res.*, 2014, **42**, 6078–6089.
- 25 A. Padirac, T. Fujii and Y. Rondelez, *Proc. Natl. Acad. Sci. U. S. A.*, 2012, **109**, E3212–E3220.
- 26 H. W. H. van Roekel, L. H. H. Meijer, S. Masroor, Z. C. Félix Garza, A. Estévez-Torres, Y. Rondelez, A. Zagaris, M. A. Peletier, P. A. J. Hilbers and T. F. A. de Greef, *ACS Synth. Biol.*, 2015, **4**, 735–745.
- 27 J. Kim and E. Winfree, *Mol. Syst. Biol.*, 2011, **7**, 465.
- 28 E. Franco, E. Friedrichs, J. Kim, R. Jungmann, R. Murray, E. Winfree and F. C. Simmel, *Proc. Natl. Acad. Sci. U. S. A.*, 2011, **108**, E784–E793.
- 29 M. Weitz, J. Kim, K. Kapsner, E. Winfree, E. Franco and F. C. Simmel, *Nat. Chem.*, 2014, **6**, 295–302.
- 30 K. Montagne, R. Plasson, Y. Sakai, T. Fujii and Y. Rondelez, *Mol. Syst. Biol.*, 2011, **7**, 466.
- 31 T. Fujii and Y. Rondelez, *ACS Nano*, 2013, **7**, 27–34.
- 32 S. N. Semenov, A. S. Y. Wong, R. M. van der Made, S. G. J. Postma, J. Groen, H. W. H. van Roekel, T. F. A. de Greef and W. T. S. Huck, *Nat. Chem.*, 2015, **7**, 160–165.
- 33 H. Niederholtmeyer, V. Stepanova and S. J. Maerkl, *Proc. Natl. Acad. Sci. U. S. A.*, 2013, **110**, 15985–15990.
- 34 E. Karzbrun, A. M. Tayar, V. Noireaux and R. H. Bar-Ziv, *Science*, 2014, **345**, 829–832.
- 35 Y. Wei, P. J. Wesson, I. Kourkine and B. A. Grzybowski, *Anal. Chem.*, 2010, **82**, 8780–8784.
- 36 M. M. Wrobel, T. Bansagi, S. K. Scott, A. F. Taylor, C. O. Bounds, A. Carranza and J. A. Pojman, *Biophys. J.*, 2012, **103**, 610–615.
- 37 D. G. Míguez, V. K. Vanag and I. R. Epstein, *Proc. Natl. Acad. Sci. U. S. A.*, 2007, **104**, 6992–6997.
- 38 M. Loose, E. Fischer-Friedrich, J. Ries, K. Kruse and P. Schwille, *Science*, 2008, **320**, 789–792.
- 39 V. Ivanov and K. Mizuuchi, *Proc. Natl. Acad. Sci. U. S. A.*, 2010, **107**, 8071–8078.
- 40 S. N. Semenov, A. J. Markvoort, W. B. L. Gevers, A. Piruska, T. F. A. de Greef and W. T. S. Huck, *Biophys. J.*, 2013, **105**, 1057–1066.
- 41 X. Liao, R. T. Petty and M. Mrksich, *Angew. Chem., Int. Ed.*, 2011, **50**, 706–708.
- 42 S. N. Semenov, A. J. Markvoort, T. F. A. de Greef and W. T. S. Huck, *Angew. Chem., Int. Ed.*, 2014, **53**, 8066–8069.
- 43 M. Isalan, C. Lemerle and L. Serrano, *PLoS Biol.*, 2005, **3**, e64.
- 44 J. S. McCaskill and G. J. Bauer, *Proc. Natl. Acad. Sci. U. S. A.*, 1993, **90**, 4191–4195.
- 45 A. Padirac, T. Fujii, A. Estévez-Torres and Y. Rondelez, *J. Am. Chem. Soc.*, 2013, **135**, 14586–14592.
- 46 S. M. Chirieleison, P. B. Allen, Z. B. Simpson, A. D. Ellington and X. Chen, *Nat. Chem.*, 2013, **5**, 1000–1005.
- 47 T. Pellinen, T. Huovinen and M. Karp, *Anal. Biochem.*, 2004, **330**, 52–57.
- 48 K. Pardee, A. A. Green, T. Ferrante, D. E. Cameron, A. DaleyKeyser, P. Yin and J. J. Collins, *Cell*, 2014, **159**, 940–954.
- 49 R. Fernandes, V. Roy, H.-C. Wu and W. E. Bentley, *Nat. Nanotechnol.*, 2010, **5**, 213–217.
- 50 R. Lentini, S. P. Santero, F. Chizzolini, D. Cecchi, J. Fontana, M. Marchioretto, C. Del Bianco, J. L. Terrell, A. C. Spencer, L. Martini, M. Forlin, M. Assalg, M. D. Serra, W. E. Bentley and S. S. Mansy, *Nat. Commun.*, 2014, **5**, 4012.
- 51 X. He, R. S. Friedlander, L. D. Zarzar and J. Aizenberg, *Chem. Mater.*, 2013, **25**, 521–523.

